

# Design and Simulation of a Fixed-wing Zagi-type UAS for the Colombian Air Force

## *Diseño y Simulación de UAS de Ala Fija Tipo Zagi para la Fuerza Aérea Colombiana*

Ing. George Mauricio Ardila Marulanda<sup>1</sup>, Ing. Juan Manuel Prieto Bohórquez<sup>1</sup>,  
 Ing. Paula Rocío Macías Castillo<sup>1</sup>, Ing. Miguel Ángel Rincón Otálora<sup>1</sup>,  
 Ing. María Betzabe Rubiano Esmeral<sup>1</sup>, Edwin Alexander Casallas Moreno<sup>1</sup>,  
 Ing. Jorge Ernesto Sánchez Rojas<sup>1,2</sup>, Ing. Daniel Felipe Cantor Santana<sup>1,2</sup>

<sup>1</sup> Fuerza Aérea Colombiana, Centro Investigación y Desarrollo Tecnológico de Innovación Aeronáutica, Madrid, Cundinamarca, Colombia.

<sup>2</sup> Universidad Nacional de Colombia, Facultad de Ingeniería, Bogotá, Bogotá D.C., Colombia.

Correspondence: [george.ardila@fac.mil.co](mailto:george.ardila@fac.mil.co)

Received: september 09, 2024. Accepted: december 27, 2024. Published: january 01, 2025.

**How to cite:** G. M. Ardila Marulanda, "Design and Simulation of a Fixed-wing Zagi-type UAS for the Colombian Air Force", RCTA, vol. 1, no. 45, pp. 91–103, jan. 2025.

Recovered from <https://ojs.unipamplona.edu.co/index.php/rcta/article/view/3226>

Copyright 2025 Colombian Journal of Advanced Technologies.

This work is licensed under a [Creative Commons Attribution-NonCommercial 4.0 International License](https://creativecommons.org/licenses/by-nc/4.0/).



**Abstract:** This study presents the design process of a Fixed-Wing Unmanned Aerial System (UAS), specifically a Zagi-type wing, for the Center for Research and Technological Development of Aeronautical Innovation (CETIA), a research center of the Colombian Air Force (FAC). The FAC recognized the need to develop its own UAS tailored to the organization's specific requirements at a time when the demand for these devices is increasing in Colombian airspace. The study begins with defining the initial specifications, selecting the electronic components related to these specifications, calculating the current consumption (A) at cruising speed and battery capacity, progressing towards the design of the fuselage, and finally selecting the aerodynamic profile of the wing and tail for Bogotá's conditions, validating the selection through CFD simulation. The research aims to address CETIA's unique operational needs within the evolving UAS landscape.

**Keywords:** Zagi wing design, remotely piloted aircraft, fixed wing, flight plan.

**Resumen:** Este estudio presenta el proceso de diseño de un Sistema Aéreo no Tripulado (UAS por sus siglas en inglés) de ala fija tipo Zagi para el Centro Investigación y Desarrollo Tecnológico de Innovación Aeronáutica (CETIA), un centro de investigación de la Fuerza Aérea Colombiana (FAC) que reconoció la necesidad de desarrollar su propio UAS adaptado a los requisitos específicos de la organización en una época en la que la demanda de estos dispositivos aumenta en el espacio aéreo colombiano. El estudio empieza con la definición de las especificaciones iniciales, la selección de los componentes electrónicos relacionados con estas especificaciones, el cálculo del consumo de corriente (A) a velocidad de crucero y capacidad de la batería, avanzando hacia el diseño del fuselaje para finalmente seleccionar el perfil aerodinámico del ala y cola para las condiciones de Bogotá, validando

su selección mediante simulación CFD. La investigación tiene como objetivo abordar las necesidades operativas únicas de CETIA en el contexto del panorama en evolución de las UAS.

**Palabras clave:** diseño de ala Zagi, aeronave piloteada remotamente, ala fija, plan de vuelo.

## 1. INTRODUCTION

Prior to now, helicopters, airplanes, or other manned aircraft were mostly used for hazardous or repetitive jobs including streamlining patrolling, tracking, and hazard assessment. This resulted in significant expenses for fuel, maintenance, and employee training [1]. Workers in restricted areas, such as military bases, frequently had to put in extended workdays in order to monitor them, being exposed to factors such as human fatigue and related work risks when operating aircrafts (*e.g., helicopter, airplane*).

Because the components of UAS are developing at a quick pace, their development has accelerated over time. For instance, multivehicle cooperative control, encrypted communication links, and GPS modules are already standard on even hobbyist drones. These qualities allow them to be employed for ground reconnaissance, albeit there are certain drawbacks as well, namely their limited ability to transport large loads and the susceptibility of unencrypted data lines and video streams to interception. Nonetheless, using more sophisticated drones—such as ones designed for the military—can increase their capacity to perform duties like border surveillance [2].

In Colombia there are two authorities in charge of overseeing the regulatory framework in the air, as mentioned next.

- The UAEAC (Unidad Administrativa Especial de Aeronáutica Civil), under the Colombian Ministry of Transport, it is the organization in charge of overseeing Colombian airspace management, civil aviation regulation, and aviation sector regulation. Additionally, Aerocivil is in charge of overseeing and administering each and every public airport in Colombia. Through the RAC (Reglamentos Aeronáuticos de Colombia), this organization imposes restrictions in these fields.
- The RAC 100, as part of the RAC, establishes the rules for operating UAS for

both commercial and non commercial uses, including requirements for operators, mandatory certifications, and operational restrictions to ensure safety and compliance with international standards [3].

- AAAES (Autoridad Aeronáutica Aviación de Estado) is the organization responsible for overseeing the aeronautical operations of the state entities, such as the police and the military through the regulatory document RACAE (Reglamento Aeronáutico Colombiano de la Aviación de Estado) [4].

First, it specifies a weight range: 0.25 kg for small drones and 0.25 kg for large drones. This regulation outlines the operational characteristics that must be met, such as the use of GPS, an identification card, low-noise motors (steel propellers are prohibited), keeping a minimum distance of less than 1.8 km from buildings owned by the government, police, military, and penal institutions, not carrying firearms or transporting animals, and requiring drone operators to have a flight license [5].

UAS have a wide range of applications in different types of industries such as agriculture, military and delivery. In agriculture UAS are used for crop management, water stress assessment, detection of pests, diseases and weeds and yield estimation [6], these activities can be carried out by different type of UAS fixed wing Zagi-type are well suited for covering wide areas efficiently, thus, monitoring of the farm conditions is done with ease [7]. In military use, UAS take an important place on reconnaissance and surveillance tasks been a complement to the existing surveillance technologies because they are equipped with cameras and AI modules for people detection. This way, those tasks are more efficient. Also, UAS can be used in military training, as aerial maneuvering targets [8], [9].

As seen by the increasing use of drones in the past, the employment of robots and autonomous machines to replace labor-intensive and hazardous tasks has increased due to their adaptability and long term affordability (*e.g., increased accessibility to difficult or dangerous areas*) [10]. The goal of this research

is to design a Zagi wing, an aircraft without tail, to carry out surveillance and reconnaissance tasks, with the implementation of Artificial Intelligence (AI) modules for reconnaissance and target tracking.

## 2. METHODOLOGY

At first, the weight and wingspan were estimated. Electronic components were chosen with the basic criteria of autonomous flight, facial recognition, excellent camera resolution, and an expected one-hour flight duration in mind.

A selection matrix with two propositions was used; the first was focused on achieving a desirable price-performance ratio, and the second was more focused on achieving outstanding performance. Subsequently, airfoils were selected comparing drag and lift performance in three of the most used NACA airfoils associated with drone applications: The NACA 4412 [11], NACA 2412 [12] and NACA 4410 [13] for the wing section and NACA 0012 [14] for the tail section, these airfoils were chosen to reduce drag forces, maximize lift, and offer stability based on particular work characteristics such as Reynolds number, Mach number, air density, and dynamic viscosity. Then, XFLR5 software was used to simulate these airfoils. Moreover, an elliptical wing contour shape with a leading edge of high eccentricity and a trailing edge of low eccentricity was selected because of its shown success, drawing inspiration from VTOL aircraft.

## 3. THEORETICAL FRAMEWORK

In this section, we will introduce some concepts related to the initial development of the Zagi wing by the Colombian Airforce subsection **Technological Center of Aeronautical Innovation (CETIA)**.

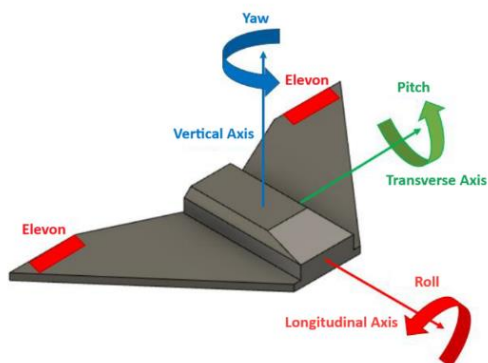


Fig. 1. Control surfaces and rotation axis of a Zagi wing.  
Source: own elaboration.

Because it merges the ailerons and elevators into a single set of surfaces, i.e., the elevons, a Zagi wing is an aircraft without a tail. Because of this, the lift and flight control principles of this aircraft are simple. These two elevons, which adjust their angle in accordance with the intended axis rotation, are what allow the airplane to move. For example, in a roll motion, the elevons move up and down in opposite directions. [15] The elevons move in the same direction during pitch motion. Yaw motion is insufficient on its own. As seen in Fig.1.

## 4. CONCEPTUAL DESIGN

Prior to starting the drone's design process, it is necessary to specify the drone's specifications and design parameters, keeping in mind limitations such as available space, resources, and production equipment, i.e., CETIA's manufacturing capabilities, taking into account that in the future the FAC is planning to do the manufacturing of the aircraft at its facilities, as one of the main goals of the FAC is to have the capacity of designing and building its own UAS.

*Requirements and design parameters of the drone*  
According to the FAC, the aircraft for its mission has to be:

- An UAS focused on reconnaissance and vigilance missions.
- A capable UAS which can help on the security and defense on air bases.
- It is needed to reduce human manipulation, in terms of supervision and piloting.

### 4.1 Requirements:

- Autonomy of at least one hour of flight time.
- A communication range of over 10 km.
- The aircraft must take off and land vertically. VTOL Tail-sitter configuration.
- The aircraft must be able to transmit, record, and save photos and videos.
- A minimum video resolution of HD (1920x1080p) and a refresh rate of 25 Hz.

In the same vein, it is necessary to establish initial design parameters for the initial calculations and selection matrix.

#### 4.1.1 Design parameters:

- For better stability the drone will have two electric motors, each of them brushless for minimum friction losses.

- The electronic circuit needs to have: A flight Controller (FC), an air unit/ air module, cameras, recording system and geolocation systems (GNSS).

#### 4.1.2 Design by selection Matrix:

Now that the requirements have been established, employing selection matrixes, as shown in tables 1, 2, 3, and 4). The alternatives for the components are:

- Optimal performance irrespective of cost considerations: Flight controller SIYI N7, communication system SIYI MK15, camera SIYI ZR30, GNSS HolyBro M9N or CUA V NEO3 PRO.
- Cost-Effective optimal performance: Flight controller SIYI N7 o HolyBro Pixhawk 6X, communication system SIYI MK15, camera SIYI A8 MINI, GNSS HolyBro M9N.

As can be seen, two options were produced: The first prioritized excellent performance in accordance with the design parameters, and the second sought a favorable price-performance ratio.

**Table 1: Flight Controllers comparison**

Criterion	Weight	PIXHAWK 6X	Cube Orange+	SIYI N7 Autopilot
Price	8	0.6	0.55	0.8
MCU Capacity	7	0.85	1	0.9
Sensors	5	0.8	0.8	0.9
Compatibility	7	0.9	0.85	0.95
Software	3	1	1	0.95
Size and Weight	6	0.5	0.8	0.85
<b>TOTAL</b>	<b>36</b>	<b>27.05</b>	<b>29.15</b>	<b>30.05</b>
<b>WITHOUT PRICE</b>	<b>28</b>	<b>22.25</b>	<b>24.75</b>	<b>27.25</b>

*Source: own elaboration.*

**Table 2: Controlllers comparison**

Criterion	Weight	SIYI MK15	SIYI MK32	Cubepilot Herelink
Price	7	0.9	0.7	0.4
Range	9	0.7	0.7	1
Channels	4	0.8	1	0.5
Control Capacity	9	0.8	0.7	0.8
FC	6	1	1	0.5
APPS	4	1	1	1
Air Unit	8	0.7	0.7	0.7
Size, Weight AU	8	0.5	0.5	0.6
Camera	2	1	0	0
<b>TOTAL</b>	<b>57</b>	<b>44.6</b>	<b>41.1</b>	<b>38.4</b>
<b>WITHOUT PRICE</b>	<b>50</b>	<b>38.3</b>	<b>36.2</b>	<b>35.6</b>

*Source: own elaboration.*

**Table 3: Comparison of cameras**

Criterion	Weight	SIYI ZR10	SIYI A8 mini	TAROT PEEPER T10X
Price	8	0.6	0.9	0.6
Quality	8	0.7	0.3	0.5
E/S	6	1	1	0.7
Size/Weight	9	0.7	0.9	0.7
Stabilization	6	0.5	0.8	0.9
<b>TOTAL</b>	<b>37</b>	<b>25.7</b>	<b>28.5</b>	<b>24.7</b>
<b>WITHOUT PRICE</b>	<b>29</b>	<b>20.9</b>	<b>21.3</b>	<b>19</b>

*Source: own elaboration.*

**Table 4: Comparison of GPS Modules**

Criterion	Price	Holybro M9N	SE100	TS100
Price	8	0.7	0.8	0.9
Capacity	10	0.9	0.8	0.5
Size/Weight	8	0.8	0.8	0.9
<b>TOTAL</b>	<b>26</b>	<b>21</b>	<b>20.8</b>	<b>19.4</b>
<b>WITHOUT PRICE</b>	<b>18</b>	<b>15.4</b>	<b>14.4</b>	<b>12</b>

*Source: own elaboration.*

After it was established the wing's components it was possibly took an initial reference for the total weight (adding each weight components plus a fuselage approximation weight). Additionally, the required space for Zagi's components was determined based on size of each component). This way the aircraft needs:

- It is needed a wingspan between 700 and 1000 mm to store the electronic components.
- Weight: Between 1 kg and 1,3 kg.

## 4.2 Motors selection

As it's said, the Zagi will take off vertically. Since the airplane is anticipated to weigh between 1 kg and 1,3 kg, the motors must be able to provide a thrust superior to the Zagi's weight, this thrust is considered to represent 50% of the motors maximal effort to provide a margin of safety.

It takes four cells with a combined voltage of 14,8 V (4S battery). The chosen motors for this configuration are the SunnySky X2216 V3 880 KV, paired with APC9045 propellers.

### 4.2.1 Electronic Speed Controllers (ESC)

The ESC selection requires calculating an ideal current ( $i_{ESC}$ ) based of its maximum capability, with a safety factor of 20%. According to the datasheet ESC can operate a 32 A motor (1). Therefore:

$$i_{ESC} = 32A \cdot 120\% = 38,4A \quad (1)$$

The TMOTOR AT55A 2-6S model was chosen, based on manufacturer's recommendation as It can handle a maximum current of 55A.

#### 4.2.2 Servomotor:

Servomotors are necessary in order to change the flying height and route during the flight i.e. For this application, EMAX ES08MA II servomotors with PWM (Pulse Width Modulation) control have been chosen. These motors are equipped with a gearbox and are necessary for aileron control.

#### 4.2.3 Battery capability:

The batteries are the responsible for the autonomy of the aircraft. Determining the aircraft's total current (I) is vital because of this. To approximate the overall current, the current for each component was computed and the results were added together. To the closest whole number, the values were rounded up. The approximation and a summary of the Zagi's total current are shown in Table 6.

**Table 5:** Required Current for electronic components

Device	Current (A)
i_Motor	5,75
i_Servo	0,5
i_cam	0,34
i_AU	1,1
i_GNSS + FC	0,3
i_Total	7,69 ≈ 7,7

Source: own elaboration.

With Table 6, it was chosen which type of batteries will be used. There are 3 alternatives: LiPo batteries, Li-Ion batteries, and graphene batteries.

Because of its large capacity and rapid charging, graphene batteries are a good choice for increased autonomy. But they cost twice as much as the aircraft itself, which is an extremely expensive price. Li-Po batteries, on the other hand, are the most popular choice, but they come with a big disadvantage. Voltage loss results from the current delivery, which raises another concern and necessitates a larger battery capacity (2):

$$Cap_{bat} = 77000mAh * 120\% = 9240mAh \quad (2)$$

This option was discarded due to the increase in weight. Li-Oin batteries are the last choice because they have the maximum energy density. The most common battery is 21 mm in diameter and 70mm in

height, with capacity of 4200 mAh. However, it is possible to boost the overall capacity, two batteries can be connected in parallel (77000 mAh). Both cells are connected in series to produce the necessary voltage of 14.8 V. This way, the type of battery that will be used is a 4S 2p Li-Ion battery.

### 4.3 Flight Parameters

The flight parameters were derived from the conceptual design of the aircraft using a specific selection matrix for each component. As a result, the initial parameters are as follows:

- Weight: Inside the 1 to 1,3 kg range, approximately 1,2 kg.
- Maximum Thrust: 2360 g.
- Battery Capacity: 10000 mAh.
- Endurance: Approximately 1 hour 15 minutes.
- Video Quality: 1920x1080p PHD at 30 FPS or 4K at 25 FPS.

### 4.4 Components list:

With the conceptual design completed, the cost of the electronic components selected were researched through a market study relevant for Colombia, the total cost and quantities of these components are summarized in Table 7.

**Table 6:** Market research of electronic components

Quantity	Component	Description	Cost (USD)
1	SIYI N7	Flight controller	\$ 279
1	SIYI MK15	Communication system	\$ 408
1	SIYI A8 MINI	Transmission camera	\$ 239
1	HolyBro M9N	GNSS system	\$ 75
2	SunnySky X2216 V3	Motors	\$ 50
2	EMAX ES08MA II	Servo motors	\$ 22
2	TMOTOR AT55A 2-6S	Electronic speed controllers	\$ 60
1	MATEK PDB-HEX	Power distribution system	\$ 27
8	INR21700 50S	Lithium-ion cells	\$ 72
<b>TOTAL</b>			<b>\$ 1,232</b>

Source: own elaboration.

Finally, Table 8 summarizes the entire matrix design, confirming the total weight, voltage, and current.

**Table 7: Component Mass and Electrical Specifications**

Component	Mass (g)	Voltage (V)	Current (A)
SIYI N7	75	5	0.3
SIYI MK15	130	16	1.1
SIYI A8 MINI	95	16	0.35
HolyBro M9N	32	5	0.15
SunnySky X2216 V3	135	16	2 x 32
EMAX ES08MA II	24	5	0.5
MOTOR AT55A	126	16	0
MATEK PDB-HEX	12	16	0
INR21700 50S	576	16	70
<b>TOTAL</b>			<b>1205</b>

Source: own elaboration.

### 4.5 Airfoil selection and analysis

To select the airfoil for the wing section firstly three NACA airfoils were compared: 4412, 4410 and 2412. The 4412 profile is a well-balanced airfoil well known in the aeronautic industry used by various aircraft manufacturer such as Aeronca, Avtech, Ayres, Bellanca and Cessna for its good performance under low to moderate Reynolds numbers, making it suitable for the Zagi wing. The 4410 is a relatively similar airfoil to the 4412 but slightly thinner, this results in less drag which is favorable but also having the tradeoff of generating less lift as well and finally, the NACA 2412 airfoil has the least camber of the three options, making it the thinnest of the comparison, generating minimum drag as well as lift, working better in higher speeds. For these three airfoils the relationship between lift coefficient (Cl) and angle of attack were compared (Fig. 1, as well as the relationship between drag coefficient (Cd) and Cl (Fig. 2), in both comparisons the airfoil selected has to be the highest in the graph.

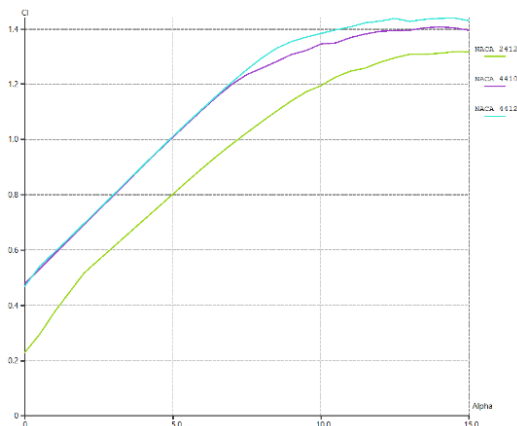


**Fig. 2. Relationship between the lift coefficient Cl with attack angle Alpha for the three proposed airfoils**  
 Source: own elaboration

As shown in the previous figures, the NACA 4412 profile performs the best in the comparison, being the highest at both graphs, this shows how well balanced the airfoil is at the operational conditions and makes it the selected option.

To be able to view the performance of the selected airfoil better the simulation is executed again using XFLR5 software. By looking at Fig. 3 it is discovered that the aircraft can produce a force 1,4 times its weight at an angle of attack of 10 degrees.

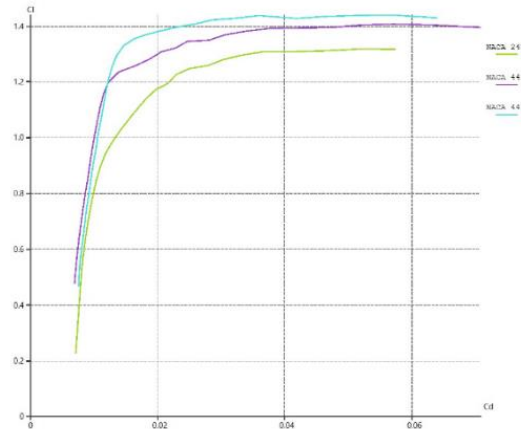


**Fig. 3. Relationship between the lift coefficient Cl and drag coefficient Cd for the three proposed airfoils.**  
 Source: own elaboration

While flying with this angle of attack and generating its respective lift, this airfoil generates only 0,02 times the aircraft weight as drag force (Fig. 4).

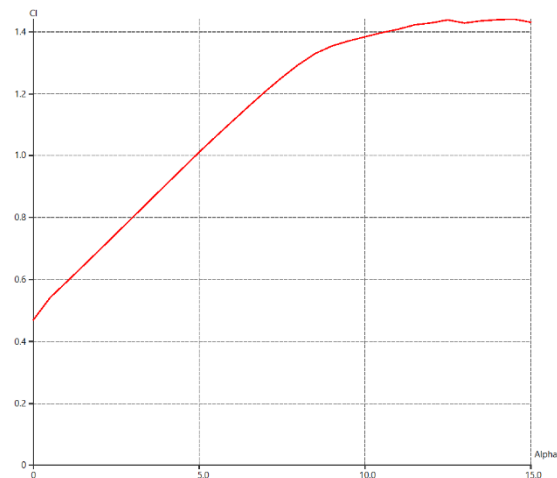


**Fig. 4. Relationship between the lift coefficient Cl with the drag coefficient Cd for NACA4412**  
 Source: own elaboration

It was decided not to run a simulation for the airfoil of the tail section because the vertical stabilizer has a NACA 0012 as the selected profile, a symmetric

airfoil with the sole objective of stabilizing the aircraft due to generating equal forces in both sides.

**5. RESULTS AND DISCUSSION**

Now conceptual design was completed, and initial considerations were established. It was time to focus on detailed design, this includes the wing’s parametrization, the CAD design of the aircraft, and its simulation on ANSYS Fluent. As can be seen:

**5.1 Detailed design**

*5.1.1 Wing cone parametrization*

The NACA 4412 profile was chosen in the search for the best airfoil because of its track record of performance in a variety of settings. On the other hand, the symmetrical NACA 0012 profile was selected for the vertical stabilizer in order to provide equal lift forces on both sides.

The following equations elucidate the mathematical formulation governing the wing's outline and design:

*Leading Edge*

$$x = 500 \cdot \cos(t), 0 < t < 2\pi \quad (3)$$

$$y = 125 + |50 \sin(t)|, 0 < t < 2\pi \quad (4)$$

*Trailing Edge*

$$x = 500 \cdot \cos(t), 0 < t < 2\pi \quad (5)$$

$$y = -45 - |130 \cdot \sin(t)|, 0 < t < 2\pi \quad (6)$$

The wing contour was generated using parametrization equations (from (3) to (6)). The resulting Fig. 5 illustrates the form of the parametrization.

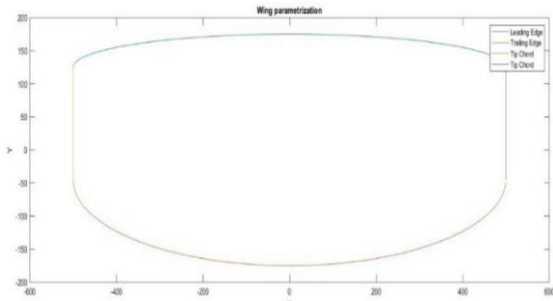


**Fig. 5. Airfoil parametrization**  
 Source: own elaboration

After that, it was time to use Fusion 360 to model the airfoil. On the basis of the model, estimated weight estimations for the aircraft were then made. The results showed that the wingspan should have been adjusted to 1,2 meters.



**Fig. 6. Vertical stabilizer design**  
 Source: own elaboration

In terms of vertical stabilization, it was imperative to endow it with the capability to provide support during VTOL (Vertical Take-Off and Landing) maneuvers. This enhancement is illustrated in Fig. 6.

*5.1.2 Fuselge Design*

*External design:* The fuselage design prioritizes aerodynamics while accommodating all electronic components, leading to dimensions of 0,2 meters by 4,65 meters and a maximum height of 0,15 meters (Fig. 7).



**Fig. 7. Fuselage design**  
 Source: own elaboration

*Internal design:* Considering the substantial size of the aircraft, the design concept was segmented into parts, as illustrated in Fig. 8. This approach aims to streamline the manufacturing process. Additionally, the plan calls for using a mobile platform to align the center of mass and simplify the assembly geometry for the electronic components.

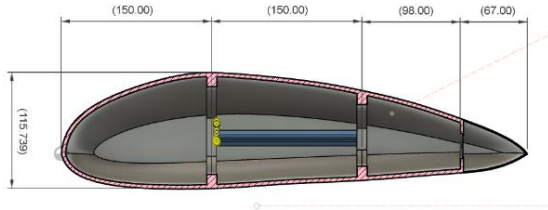


**Fig. 8. Fuselage sections**  
 Source: own elaboration

5.1.3 Surface finishes

For the vertical wing, which does not enclose any internal components, it simply needs to be affixed beneath the fuselage. Therefore, the junctions between sections must be as seamless as possible to minimize turbulent airflow and optimize flight efficiency.

5.1.4 Assembly

A total of 8 components were designed: two ailerons, two elevons, three fuselage pieces, and a vertical stabilator. The proposed assembly method involves utilizing screwed joints for each part of the fuselage. Each module was designed with the spaces for the couplings to facilitate this assembly method (Fig. 9).

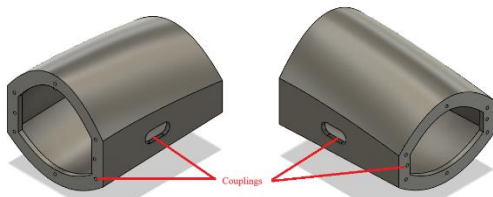


**Fig. 9. Couplings.** Source: own elaboration

The wings were assembled using an adjustment coupling with two rods: one rod located in the body of the fuselage and the other inside the wing (Fig. 10).

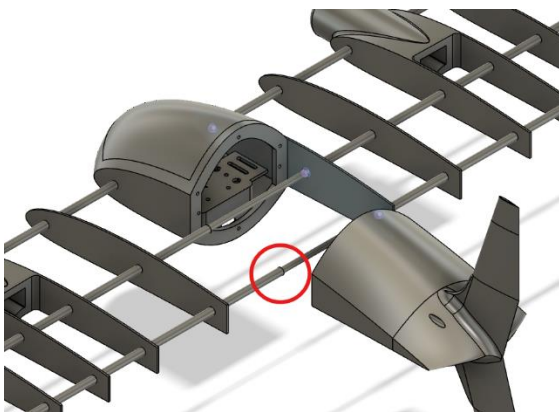


**Fig. 10. Assembly of the fuselage**  
 Source: own elaboration

Regarding the electronic components, the plan entails employing a platform capable of being displaced inside the fuselage to adjust the center of mass (Fig. 11), thus ensuring the aircraft achieves stable flight.

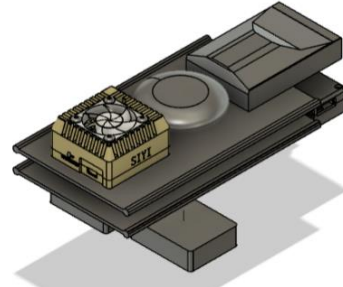


**Fig. 11. Electronic Assembly**  
 Source: own elaboration

5.1.5 Motor Mount

To accommodate the motor assemblies, two cylindrical mounts were designed at the front of the wing, with one on each side for each motor. These mounts play a crucial role during VTOL takeoff. Furthermore, considerable efforts were dedicated to ensuring a smooth surface interaction with the wing.

5.1.6 Simulations

With the objective of predicting the aircraft's behavior under typical weather conditions in Bogotá (with dynamic viscosity and air density values of  $1,42 \times 10^{-5} \text{ Pa} \cdot \text{s}$  and  $0,895 \text{ kg/m}^3$ , respectively) [16], and a velocity of  $16,66 \text{ m/s}$ , Computational Fluid Dynamics (CFD) simulations were conducted using Ansys Fluent software. Consequently, a computational domain size of  $1 \times 1.5 \times 1.6 \text{ m}$  was chosen, as detailed analysis of airflow far from the aircraft was deemed unnecessary. The initial objective is to evaluate the aircraft's performance across various metrics, including lift force, drag force, pressure coefficient, and turbulent kinetic energy. Table 8 depicts the specific parameters governing the mesh structure employed within the computational framework. Tetrahedral elements were judiciously selected to accommodate the intricate and multifaceted geometric nuances inherent in the aircraft's design. This choice of tetrahedral geometry facilitates an accurate representation of the complex three-dimensional spatial characteristics essential for comprehensive simulation analysis.



**Table 8: Mesh parameters**

Mesh size	
Element size [m]	0.45
Maximum element size [m]	0.9
Deformation size [m]	2.25E-03
Minimum curvature size [m]	4.50E-03
Curvature angle [°]	18
Smoothing	Medium
Growth	
Transition rate	0.272
Maximum number of layers	5
Growth rate	1.2
Statistics	
Nodes	87245
Elements	486639

Source: own elaboration

With an initial angle of attack of 0° and a calculated Reynolds number of 362410, the lift force was determined to be 14,811858 N, while the drag force was found to be 1,2743155 N. To gain insight into the airflow characteristics near the aircraft, Fig. 12 and Fig. 13 depict the contours of pressure coefficient and turbulent kinetic energy, respectively.

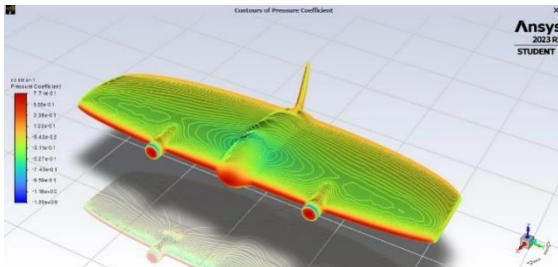


Fig. 12. Contours of pressure coefficient at 0° AoA  
 Source: own elaboration

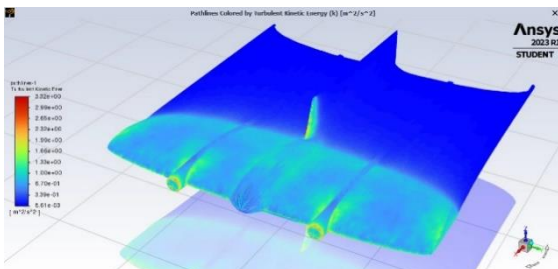


Fig. 13. Turbulent kinetic energy at 0° AoA  
 Source: own elaboration

Upon examination of the lift force generated at an angle of attack of 0°, it becomes apparent that an aircraft with a maximum weight of 1,51 kg is capable of maintaining flight under this condition. However, given that the anticipated weight range for the aircraft is between 1 and 1,3 kg, it is evident that these values are closely clustered, heightening the risk of stalling. In light of this, further analysis was conducted on the aircraft's behavior at an angle of attack of 10° (Fig. 14 and Fig. 15). Subsequently, the

lift force and drag force were calculated to be 52,45 N and 5,53 N, respectively.

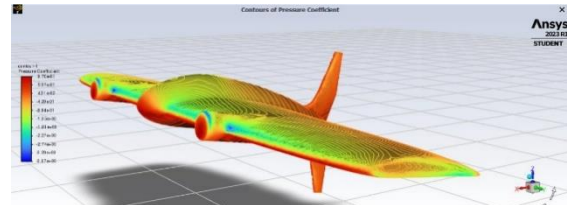


Fig. 14. Contours of pressure coefficient at 10° AoA  
 Source: own elaboration

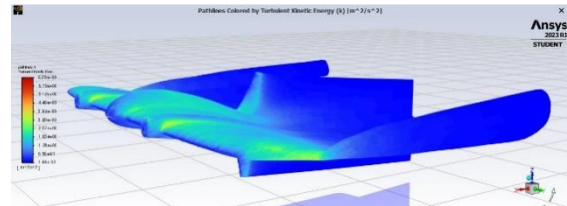


Fig. 15. Turbulent kinetic energy at 10° AoA  
 Source: own elaboration

5.1.7 Load analysis

The fuselage design, as shown previously in Fig. 9, must be validated using the aerodynamic forces calculated through simulation, particularly focusing on Section Two of the fuselage. This section is where the wings will be attached, making it the primary area responsible for withstanding both drag and lift forces, along with their resulting moments (Fig. 16).

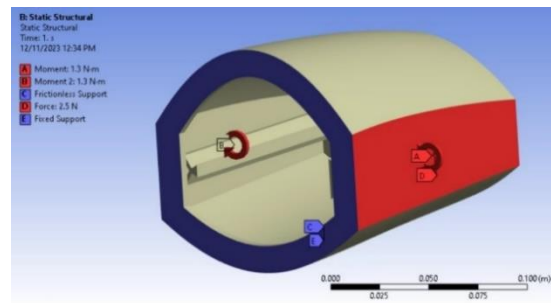


Fig. 16. Definition of loads and moments  
 Source: own elaboration

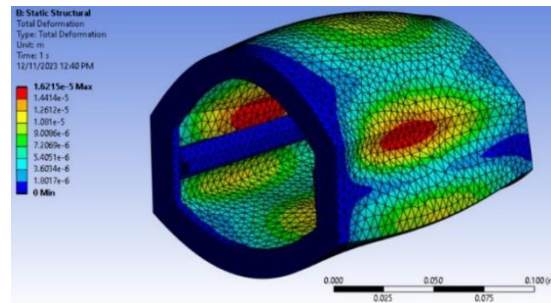
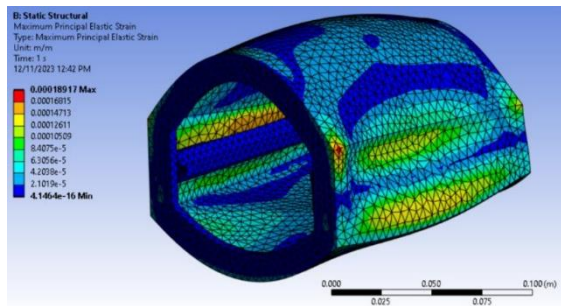


Fig. 17. Total deformation over aircraft fuselage  
 Source: own elaboration



**Fig. 18.** Maximum principal elastic strain over aircraft fuselage  
 Source: own elaboration

As illustrated in the preceding two figures (Fig. 17 and Fig. 18), the deformations and strains observed in this fuselage section are minimal, yielding a safety factor exceeding 10 when employing Onyx (by Markforged) as the manufacturing material. This indicates the design's capacity to withstand aerodynamic forces, although such outcomes may vary depending on modifications made during the manufacturing process.

**5.1.8 Manufacturing proposals**

After evaluating four options for the aircraft structure, including additive manufacturing, composite structures with carbon and aramid, cutting of extruded polystyrene, and the use of composite materials, the chosen approach was a combination of composite materials and additive manufacturing. This means that the aircraft's structure will be 3D-printed, specifically employing a rib structure and carbon fiber for the tubular section. Additionally, the wing will be reinforced with Kevlar (Fig. 19).

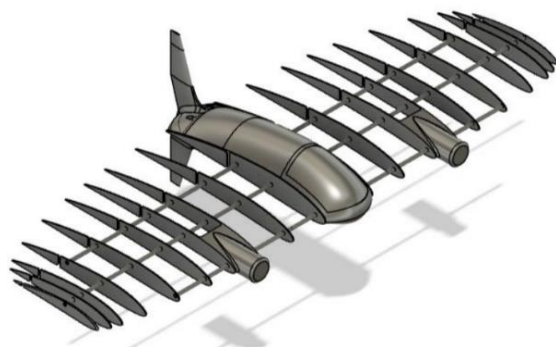


**Fig. 19.** Aircraft structure-final prototype  
 Source: own elaboration

At the Tables 9, 10, 11 are the specifications of the manufacturing materials.

**Table 9:** Composite Materials Specifications. The Onyx variants

	Onyx	Onyx FR	Onyx ESD	Nylon
Tensile modulus (GPa)	2.4	3	4.2	1.7
Tensile stress at yield (MPa)	40	41	52	51
Tensile strenght at break (MPa)	37	40	50	36
Tensile elongation at break (\%)	25	18	25	150
Flexure strenght (MPa)	71	71	83	50
Flexure modulus (GPa)	3	3.6	3.7	1.4
Thermal deflection temperature(°C)	145	145	138	41
Flame resistance UL94	V-02	-	-	-
Izod impact test – with notch (J/m)	330	-	44	110
Surface resistance ANSI/ESD STM 11.11^3	-	-	10^5 – 10^7	-
Density (g/cm3)	1.2	1.2	1.2	1.1

Source: own elaboration

**Table 10:** Mechanical properties of extruded polystyrene

Concept	Value	Standard
Long-term compression strength for maximum 2\% strain (kPa)	95	EN 1606
Compression strength (kPa)	CS(10/Y) 300	EN 826
Tensile strength perpendicular to faces (kPa)	NPD	-

Source: Composites Materials Datasheet, Markforged Corporation (October 2023) [17]

**Table 11:** Elastic Modulus of aramid epoxy

Material	Elastic Modulus (GPa)		10^6 psi	
	Longitudinal	Transverse	Longitudinal	Transverse
Aramid epoxy resin matrix fibers	76	5.5	11	0.8
High modulus carbon fibers - epoxy	220	6.9	32	1
E-glass fiber – epoxy matrix	45	12	6.5	1.8

Source: own elaboration

**5.2 Flight routes**

One of the project's aims is to enable the aircraft to autonomously navigate a predetermined route for testing purposes. In this context, GPS (Global Positioning System) and RTK (Real Time Kinematic<sup>1</sup>) play crucial roles in ensuring the creation of precise and efficient flight paths. Additionally, Table 12 summarizes the key considerations for terrain analysis in this work, including camera megapixels, vision range, and captured area.

**Table 12: Camera Specifications**

Camera (Mpx)	FOV (°)	Captured Area (m <sup>2</sup> ) at 100m Altitude	Captured Area (m <sup>2</sup> ) at 200m Altitude
6	70	150	300
12	78	200	400
16	82	250	500
20	84	300	600
24	90	400	800
30	94	500	1000

*Source: [18]*

As shown in Table 13, the FOV (Field of View) significantly impacts the quality of the captured image. Higher altitudes allow for a broader area to be captured, albeit with a reduction in image quality. Conversely, lower flight altitudes result in a smaller area being captured but yield higher-quality images.

In addition to the aircraft's altitude, its velocity also impacts the sharpness of the captured images. Higher velocities may result in blurred images, while lower velocities increase energy requirements. Furthermore, the camera angle influences how the images represent the location, potentially leading to misconceptions about the area. However, it's crucial to note that the final image quality is also contingent upon lighting conditions, weather, and the topography of the area.

To minimize flight time and costs, the route needs to be generated with the least possible redundancy while covering all the necessary areas, for the trajectory optimization it is needed to adapt the height of the flight due to territory variability, avoiding trees, buildings and related.

When a flight route is established, it is necessary to define the most efficient trajectory among a lineal, a radial, an orbital, or oblique trajectory, or to use waypoints. All have their advantages and disadvantages, depending on the trajectory intention.

### 5.2.1 Possible applications

With aircraft design and passed the Ansys Simulation. The following applications are possible scenarios where the Zagi will be used by the FAC:

- **Vigilance and territorial surveillance:** The Zagi wing is suitable for such activities due to its components. For example, the camera incorporates an AI module capable of recognizing faces, objects, and patterns. Additionally, a nocturnal camera can be installed if necessary. An ideal IRS system.

- **Environmental Monitoring:** The Zagi wing proves invaluable in monitoring deforestation zones, disaster areas, and bodies of water. Its versatility allows for effective observation and data collection in various environmental contexts, aiding in conservation efforts and disaster response.
- **Reconnaissance of special zones:** The Zagi wing is adept at conducting reconnaissance in various critical areas such as border patrolling, military base inspections, and surveillance of strategic points or tracking.
- **Inter institutional collaboration:** The Zagi wing facilitates collaboration between various organizations, such as the Army, and the Navy.
- **Security Operations:** Ideal for counterinsurgency, antidrug, and antiterrorist operations, particularly for areas with a high security risk or challenging environmental conditions.
- **For sales:** Generated design can be offered to civilians for various applications, such as topography, photograph tasks, entertainment, and more.

## 6. CONCLUSIONS

- It is evident that the most suitable attack angle for the wing is 10° concerning horizontal as this angle results in a fivefold increase in lift force. This angle also results in a fivefold increase in the thrust force, but it is not important for the aircraft's performance.
- The Ansys Fluent simulation confirms that the wing is capable of performing FAC missions under Bogota's weather conditions and surroundings.
- The Ansys Fluent simulation confirms that the wing is capable of performing FAC missions under the weather conditions of Bogotá and its surroundings.

## 7. CONFLICT OF INTEREST

The authors confirm that this work has not been used or published elsewhere. The authors also confirm that there are no conflicts of interest.

### REFERENCES

- [1] S. K V, S. Sujitha, M. D. Raman and S. Kanaujia, "Silent Surveillance Autonomous Drone For Disaster Management And Military Security Using Artificial Intelligence", in 2023 3rd International Conference on Innovative Practices in Technology and Management (ICIPTM), pp. 1–4, Feb 2023, doi: 10.1109/ICIPTM57143.2023.10118136
- [2] K. Sayler, "A WORLD OF PROLIFERATED DRONES: A Technology Primer". Center for a New American Security, 2015. Accessed 12 Apr. 2024.
- [3] Aerocivil, "RAC 100: operación de sistemas de aeronaves no tripuladas UAS," 2024. Available: <https://www.aerocivil.gov.co/normatividad/RAC/RAC>
- [4] A. A. de Aviación de Estado Fuerza Aérea Colombiana AAAES, "RACAE91 reglas de vuelo y operación," 2020. Available: <https://aaaes.fac.mil.co/sites/aaaes/files/AAAES/documentos/racae91reglasdevueloyoperacion0.pdf>
- [5] M. E. Acuña Lizarazo, "Drones, nuevos panoramas para la aviación: Análisis comparativo de la normatividad internacional frente a la normatividad colombiana" Escuela de Postgrados de la Fuerza Aérea Colombiana, 2016.
- [6] Y. Inoue, "Satellite-and drone-based remote sensing of crops and soils for smart farming {a review," *Soil Science and Plant Nutrition*, vol. 66, no. 6, pp. 798–810, 2020.
- [7] S. M. Vinodhini, "Importance of drones in agriculture," 2024.
- [8] H. Wang, H. Cheng, and H. Hao, "The use of unmanned aerial vehicle in military operations," in *Man-Machine Environment System Engineering* (S. Long and B. S. Dhillon, eds.), (Singapore), pp. 939–945, Springer Singapore, 2020.
- [9] M. Lee, M. Choi, T. Yang, J. Kim, J. Kim, O. Kwon, and N. Cho, "A study on the advancement of intelligent military drones: Focusing on reconnaissance operations," *IEEE Access*, vol. 12, pp. 55964–55975, 2024.
- [10] P. Kozak and M. Vrsecka, "The use of drones in military conflict," in 2023 International Conference on Military Technologies (ICMT), (Brno, Czech Republic), pp. 1–6, 2023.
- [11] A. Tools, "Naca 4412," 2024. Available: <http://airfoiltools.com/airfoil/details?airfoil=naca4412-il>.
- [12] A. Tools, "Naca 2412," 2024. Available: <http://airfoiltools.com/airfoil/details?airfoil=naca2412-il>.
- [13] A. Tools, "Naca 4410," 2024. Available: <http://airfoiltools.com/airfoil/naca4digit?MNaca4DigitForm>.
- [14] A. Tools, "Naca 0012," 2024. Available: <http://airfoiltools.com/airfoil/details?airfoil=n0012-il>.
- [15] A. Creus Solé, *Iniciación a la aeronáutica*. Ediciones Díaz de Santos, April 2010.
- [16] M. P. Burgos Gutiérrez, S. Aldana Ávila, and D. J. Rodríguez Patarroyo, "Análisis del recurso energético eólico para la ciudad de Bogotá D.C. para los meses de diciembre y enero, Colombia / analysis of the wind energy resource for the Bogotá City, Colombia," *Avances Investigación en Ingeniería*, 2015. DOI: <https://doi.org/10.18041/17944953/avances.2.278>
- [17] Mark Forged, "Mark two flagship continuous fiber composite 3d printer, built to revolutionize your manufacturing operation," 2023. Available: <https://markforged.com/>

- [18] B. Tikaret, “Aramida dtex 1580,” 2024.  
Available:  
<https://novarchem.com.ar/storage/app/uploads/public/5c1/1b9/486/5c11b94864079258519029.pdf>